

Article

Cylindrical Rod Phosphor Structure for Laser-Driven White Lighting

Bing-Mau Chen ¹, Shang-Ping Ying ^{1,*} , Hsuan-Li Huang ¹ and Yu-Chieh Cheng ²

¹ Department of Semiconductor and Electro-Optical Technology, Minghsin University of Science & Technology, 1, Xinxing Road, Xinfeng, Hsin-Chu 30401, Taiwan

² Department of Orthopedics, Tungs' Taichung MetroHarbor Hospital, Taichung City 435, Taiwan

* Correspondence: sbying@must.edu.tw

Abstract: In this article, a cylindrical rod phosphor structure was developed and used for laser-driven white lighting. The blue light emitting from the laser diode (LD) with limited divergence enters the cylindrical rod containing phosphor and excites the yellow phosphor particles in the cylindrical rod to generate white light. Multiple phosphor blends with yellow and red phosphors were also applied to the cylindrical rod phosphor structure to enhance the red luminescence of white light with a low correlated color temperature (CCT). An advanced structure with a surrounding transparent layer around the central cylindrical rod containing phosphors was also investigated to enhance the possibility of the blue light absorption by phosphors in the cylindrical rod region away from the LD. The cylindrical rod phosphor structures with or without the surrounding transparent layer were fabricated to produce laser-driven white lighting, and the optical characteristics of the cylindrical rod phosphor structures with different phosphor concentrations or yellow-to-red phosphor weight ratios were examined.

Keywords: laser-driven white lighting; cylindrical rod; correlated color temperature (CCT); scattering



Citation: Chen, B.-M.; Ying, S.-P.; Huang, H.-L.; Cheng, Y.-C.

Cylindrical Rod Phosphor Structure for Laser-Driven White Lighting. *Coatings* **2022**, *12*, 1637. <https://doi.org/10.3390/coatings12111637>

Academic Editor: Saulius Grigalevicius

Received: 27 September 2022

Accepted: 26 October 2022

Published: 28 October 2022

Publisher's Note: MDPI stays neutral with regard to jurisdictional claims in published maps and institutional affiliations.



Copyright: © 2022 by the authors. Licensee MDPI, Basel, Switzerland. This article is an open access article distributed under the terms and conditions of the Creative Commons Attribution (CC BY) license (<https://creativecommons.org/licenses/by/4.0/>).

1. Introduction

Solid-state lighting (SSL) is highly efficient, reliable, and environment-friendly and has thus advanced rapidly over the last decade and has been used in various applications in the lighting market. As the most successful representative of SSL, the phosphor-converted LED (pc-LED) has been extensively applied in the field of general lighting. However, the efficiency of the pc-LED decreases at high input power density, thereby limiting the performance of pc-LED in high-brightness applications [1–3]. With notable differences in the LEDs, laser diodes (LDs) primarily operate through stimulated emission without a severe decrease in efficiency when they exceed the threshold [4,5]. The use of multiple LDs of differing emission wavelengths is one approach to SSL [6]. However, the three or four discrete laser lines (red–green–blue or red–yellow–green–blue) cannot fill the visible spectrum for white light, and they cannot properly render the colors of objects. Multi-wavelength LDs with a wavelength span beyond the capability of a single laser material are important for laser-driven white light. A single LD capable of lasing at all three elementary colors from single monolithic multi-segment heterostructure nanosheets (MSHNs) in the blue, green, and red color bands is demonstrated [7]. However, the complex fabrication of MSHNs prevents the use of the application for laser-driven white light at the present stage. Besides multiple LDs, the laser-driven, phosphor-converted white light is an emerging technology with huge potential for widespread applications in SSL. However, conventional phosphor converters composed of phosphor and organic resins (silicone or epoxy) used to fabricate conventional pc-LEDs are not suitable for laser-driven white light for high-brightness applications due to the overheating and carbonization of silicone or epoxy under exposure to heat generated by laser irradiation [8–10]. The degradation of a phosphor-silicon mixture is responsible for the reduction in long-term reliability, luminous efficacy degradation, and shift of chromaticity of laser-driven white light [11,12]. A novel design

of a phosphor converter involving the application of phosphor to silicone is necessary for preventing the degradation of phosphor–silicon mixture for the laser-driven, phosphor-converted white light. An LD-based white light engine that uses a light guide design in combination with a reflective-type remote phosphor is used to improve the overall performance of the laser-based white light source [12]. The collimated LD light beam is coupled from the output end of the light guide through total internal reflection (TIR) to the reflective-type remote phosphor. The light emerging from the output end of the light guide is uniformly distributed when the phosphor plate is excited. The structure of a rotating wheel covered with colored phosphor layers excited by blue LDs is an efficient solution that provides high-output power [13–15]. However, the moving parts inside this structure limit its applicability for illumination. A ring remote phosphor (RRP) structure comprising an inverted-cone-lens encapsulant and a surrounding phosphor layer was also developed for laser-driven white lighting [16]. The encapsulant in the structure redirects light from a blue LD to the surrounding phosphor layer, thereby preventing intense light from hitting the phosphor layer on a small surface and, therefore, from considerably reducing luminous efficiency. A phosphor-coated, cylindrical-rod-based extended white light source has also been proposed [17]. The proposed extended white light source is composed of a transparent rod covered with yellow phosphor and excited by a blue LD. The laser beam is focused on the center of the front surface of the transparent rod and propagates through the rod because of TIR. Then, blue light from the LD excites the yellow phosphor in the phosphor layer around the transparent rod. However, the uniformity of the phosphor-coated, cylindrical-rod-based extended white light source is low. Variable grinding, as well as making a hollow core inside the transparent rod or gradient ground and nanoparticles inserted into the surrounding phosphor layer, was used to improve the uniformity of white light. However, precision grinding, drilling, and gradient grinding are complex processes. Moreover, the blue laser beam propagates through the entire transparent rod and escapes from the end surface of the rod without exciting the yellow phosphor. Thus, a mirror at the end of the transparent rod is necessary for confining the blue laser beam inside the transparent rod to increase the conversion efficiency of the surrounding phosphor layer.

To overcome the limitations of the phosphor-coated, cylindrical-rod-based extended white light source, a cylindrical rod containing yellow phosphor for laser-driven white lighting was evaluated in this study, as displayed in Figure 1a. Without the use of a focal lens, the blue light emitting from the LD with limited divergence enters the cylindrical rod and excites the yellow phosphor particles in the cylindrical rod to generate white light. The scattering of the yellow phosphor in the cylindrical rod results in the scattering of the blue and yellow light propagating in the rod, thereby resulting in uniform illumination [18,19]. Thus, the additional grinding and drilling of the cylindrical rod are ignored. The yellow phosphor with different phosphor concentrations that distributed uniformly in the cylindrical rod was investigated to determine the output power and correlated color temperature (CCT) of laser-driven white lighting. However, the scattering of the yellow phosphor in the cylindrical rod may also prevent the blue light from the LD from exciting the phosphor particles away from the LD when the phosphor concentration is high. Without the blue light excitation, the yellow emission and output power of the region in the cylindrical rod away from the LD would be low. To enhance the possibility of blue light absorption by yellow phosphor in the cylindrical rod region away from LD, a surrounding transparent layer around the central cylindrical rod was investigated, as illustrated in Figure 1b. The surrounding transparent layer redirects the blue light exiting the central cylindrical rod through TIR to the region away from the LD and then increases the possibility of blue light absorption by yellow phosphor in the central cylindrical rod. Another problem of laser-driven white light is its high CCT. Similar to the light emitted by pc-LEDs, the laser-driven, phosphor-converted white light is based on the integration of traditional broadband yellow phosphors and blue LD. However, the laser-driven, phosphor-converted white light emitted by yellow phosphor is not suitable for medical examination lighting or operating lights because of the poor performance in the red part of the spectrum and

the corresponding high CCT. Multiple phosphor blends with yellow and red phosphors could be used in laser-driven, phosphor-converted white light to enhance the red luminescence of white light with a low CCT. Therefore, we characterized the cylindrical rod containing both yellow and red phosphors for laser-driven white lighting in this study, as illustrated in Figure 1c. We also investigated the surrounding transparent layer around the cylindrical rod containing both yellow and red phosphors, as illustrated in Figure 1d. However, experimental observations revealed that multiple phosphor blends reduce the luminescence of individual phosphors and their corresponding luminous efficiency due to the reabsorption of light in pc-LEDs [20,21]. For the cylindrical rod containing yellow and red phosphors for laser-driven white lighting in this study, the structure may also exhibit low luminous efficiency due to the reabsorption of light in the structure. Therefore, certain photons emitted from yellow phosphor are absorbed by red phosphor particles in the same structure before they are extracted from the device. We propose a phosphor design involving a surrounding red phosphor layer in which yellow and red phosphors are separated for use in laser-driven white lighting. The yellow cylindrical rod and surrounding red phosphor layer are then separately illuminated by blue light emitted from the blue LD, as displayed in Figure 1e.

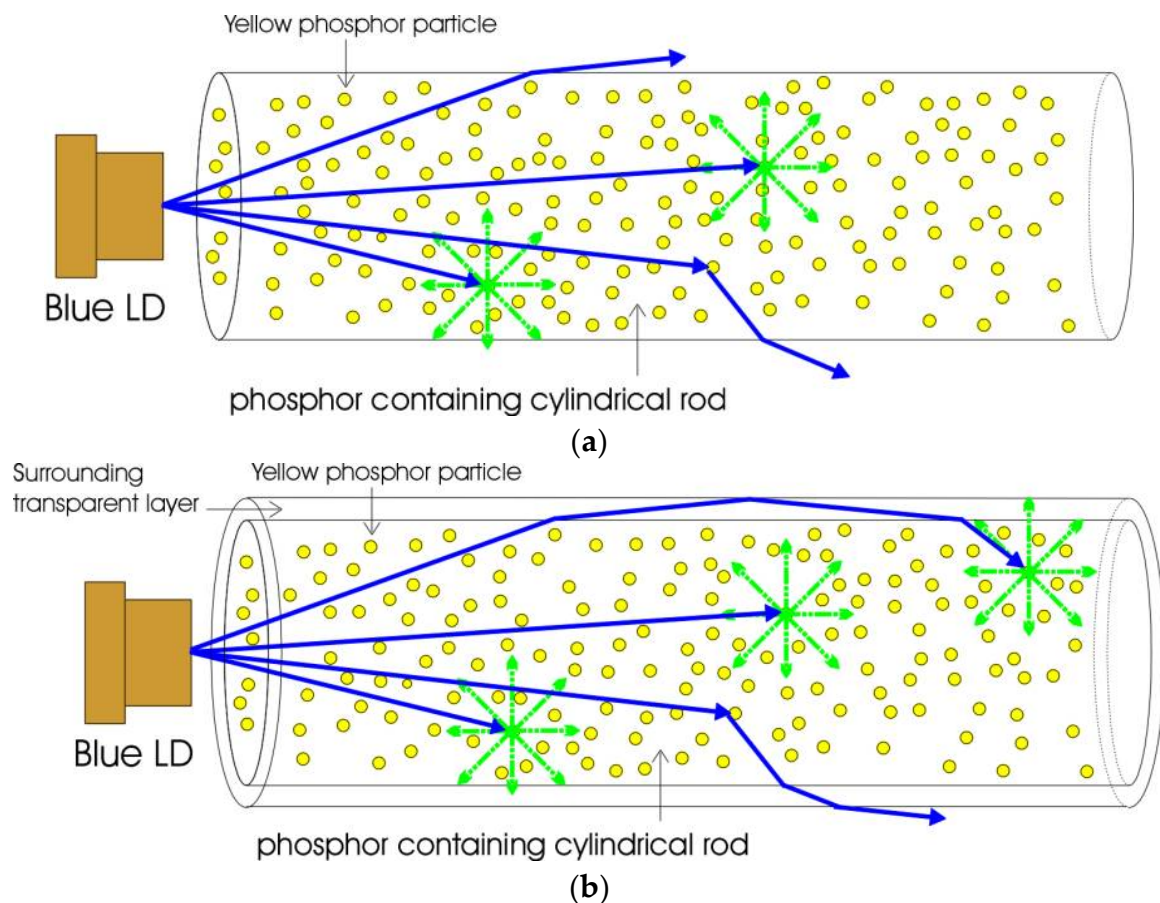


Figure 1. Cont.

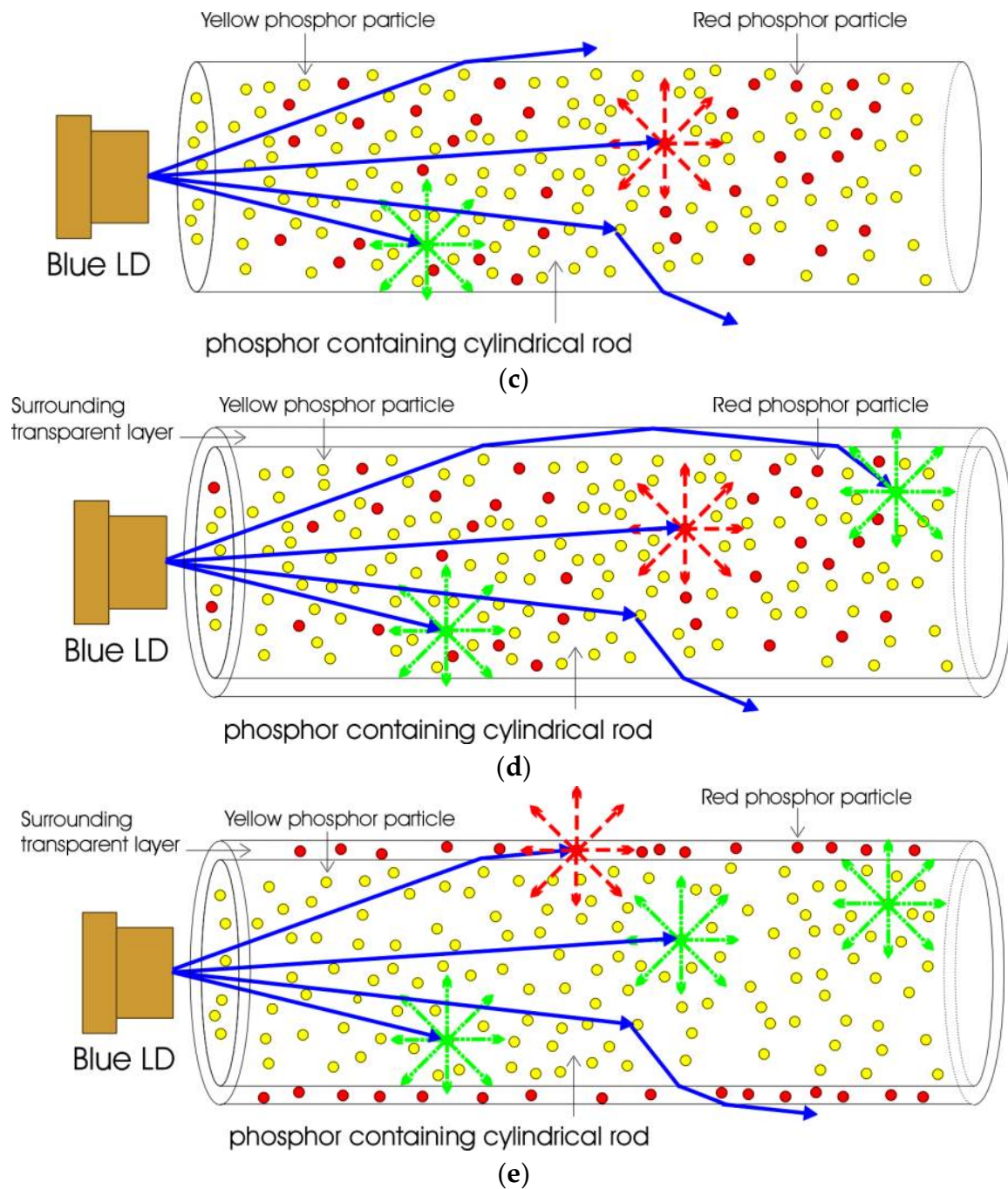


Figure 1. Schematic diagrams of (a) yellow phosphor cylindrical rod, (b) yellow phosphor cylindrical rod with surrounding transparent layer, (c) yellow and red phosphors cylindrical rod, (d) yellow and red phosphors cylindrical rod with surrounding transparent layer and (e) yellow cylindrical rod and surrounding red phosphor layer used in this study.

2. Materials and Methods

To apply the laser-driven, phosphor-converted white light, the phosphor–silicon mixture was used to fabricate the cylindrical rod containing phosphor. Figure 2 presents the process flowcharts. The yellow phosphor gel (mixture of DC-184 from Dow Corning and YAG4EL phosphor from Intematix) was injected into a cavity mold with an interior diameter of 14 mm and depth of 50 mm and then heated in an oven at 100 °C for 30 min to cure the cylindrical rod containing yellow phosphor at concentrations of 0.1%, 0.3%, 0.5%,

0.7%, and 0.9%. Then, we fabricated a yellow cylindrical rod with a diameter of 14 mm and length of 50 mm, as displayed in Figure 2b. We also fabricated a transparent layer surrounding the yellow cylindrical rod. A typical two-step molding process was used to fabricate the transparent layer surrounding the central yellow cylindrical rod. The central yellow cylindrical rod was also formed using the cavity mold with an interior diameter of 14 mm and length of 50 mm. The second step involved molding the surrounding transparent layer around the central yellow cylindrical rod. To prevent the formation of air bubbles/voids in the transparent layer, a part of the cylindrical mold with an exterior diameter of 16 mm and a depth of 50 mm was injected with transparent gel (mixture of OE-6370 HF from Dow Corning) before the central cylindrical rod was sealed in the cylindrical mold. After the central cylindrical rod was pressed up from the cylindrical mold, the transparent gel surrounded a part of the central yellow cylindrical rod. Then, we injected more transparent gel into the cylindrical mold with a needle, filling the cylindrical mold to surround the central yellow cylindrical rod, as displayed in Figure 2d. This study used 1-millimeter-thick transparent layers. After curing at 150 °C for 30 min, the fabrication of the surrounding transparent layer around the yellow cylindrical rod was completed, as displayed in Figure 2e. To apply the laser-driven, phosphor-converted white light with a low CCT, the cylindrical rod containing both yellow (YAG4EL) and red (RR6436 from Intematix) phosphors was fabricated. For the yellow phosphor (YAG4EL) concentration of 0.5%, the yellow (YAG4EL) to red (RR6436) phosphor weight ratios (Y:R) of 3:1, 6:1, 9:1, 12:1, and 15:1 were applied to the cylindrical rod containing both yellow and red phosphors. The fabrication of the cylindrical rod samples containing two phosphors was similar to that of the cylindrical rod containing yellow phosphor only. Thus, the cylindrical rod samples containing two phosphors without or with the surrounding transparent layer were obtained, as illustrated in Figure 2b,e. The red phosphor layer around the central yellow cylindrical rod sample (Figure 1e) was also fabricated through a two-step molding process. After the fabrication of the central yellow cylindrical rod with a diameter of 14 mm and a length of 50 mm, the central yellow cylindrical rod was sealed in the cylindrical mold filled with red phosphor gel (mixture of OE-6370 HF from Dow Corning and RR6436 phosphor from Intematix) and then pressed up from the cylindrical mold to surround the central yellow cylindrical rod, as illustrated in Figure 2f. At the selected yellow (YAG4EL) phosphor concentration of 0.5%, the weights of the yellow phosphor in the central yellow cylindrical rod and red phosphor in the surrounding red phosphor layer were the same as those of the phosphors used in the cylindrical rod containing both yellow and red phosphors, and the Y:R ratios were maintained at 3:1, 6:1, 9:1, 12:1 and 15:1, respectively. The thickness of the red phosphor layers was also set to 1 mm. After curing at 150 °C for 30 min, the fabrication of the surrounding red phosphor layer surrounding the central yellow cylindrical rod was complete, as illustrated in Figure 2g. For laser-driven, phosphor-converted white light with a low CCT using the same yellow phosphor concentration, the fabricated cylindrical rod containing both yellow and red phosphors or the surrounding red phosphor layer around the central yellow cylindrical rod contained the same amount of yellow phosphor, red phosphor, and silicone gel. The cylindrical rod samples with all different structures are illustrated in Figure 3a. To determine the optical characteristics of the cylindrical rod sample for laser-driven white lighting, the cylindrical rod sample was mounted on a blue LD (OSRAM PL TB450) operating at a peak wavelength of 450 nm and with a current of 350 mA, as depicted in Figure 3b. The corresponding input power was approximately 1.3 W. The blue LD was modeled using the full-width at half-maximum (FWHM) value of the Gaussian function. The divergence angles along the perpendicular and parallel transverse directions of the LDs were not identical. The FWHM values of the PL TB450 LD along each direction were assumed to be 23° and 6° [22]. The optical characteristics of the cylindrical rod samples were evaluated using an Agilent E3634A and a high-resolution spectrometer (Tristan USB) equipped with a 30 cm integrating sphere.

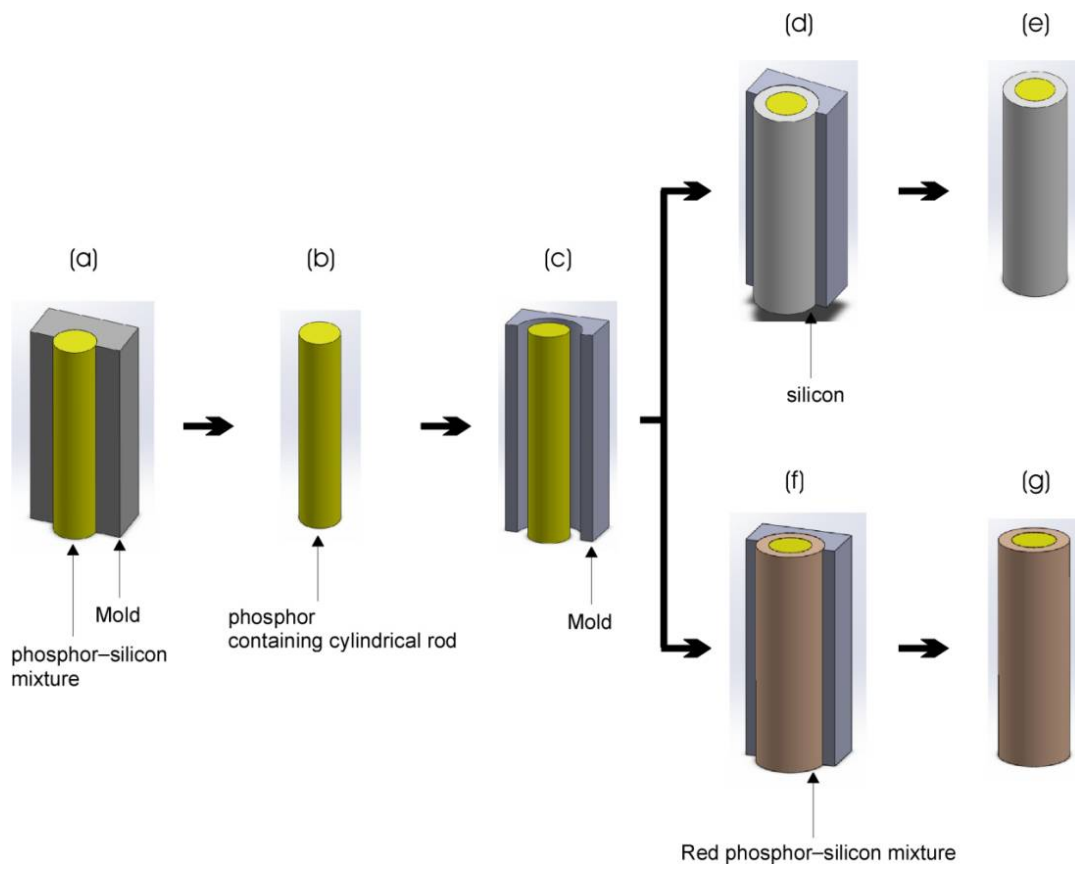


Figure 2. Schematic diagram of process flow charts in this study.

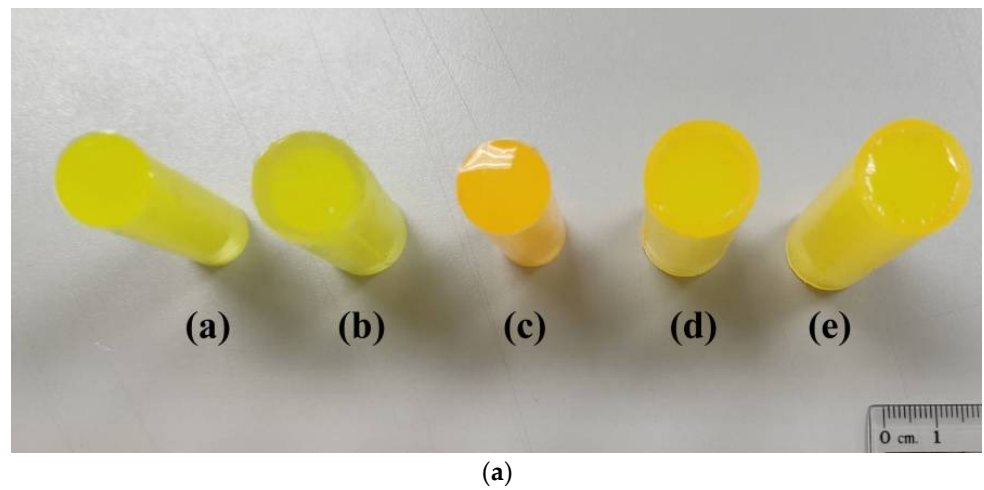
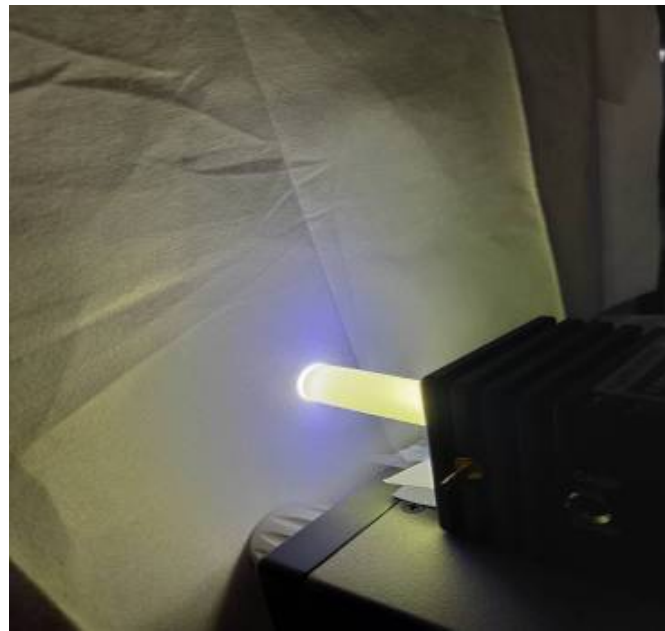


Figure 3. Cont.



(b)

Figure 3. Photographs of (a) all the cylindrical rod samples and (b) cylindrical rod containing yellow phosphor for laser-driven white lighting in this study.

3. Results and Discussion

Table 1 summarizes the optical characteristics of the cylindrical rod containing yellow phosphor with or without the surrounding transparent layer at different phosphor concentrations. The luminous fluxes of the cylindrical rod containing yellow phosphor with or without the surrounding transparent layer initially increased with the phosphor concentration and then decreased. Thus, a threshold yellow phosphor concentration was present. The human eye is more sensitive to yellow emission than to blue light, and a yellow cylindrical rod with a higher phosphor concentration exhibits a higher luminous flux, as depicted in Figure 4a,b. For yellow phosphor concentrations greater than the threshold concentration, the high scattering of phosphor prevents the yellow light emitted from the phosphor particles from escaping the yellow cylindrical rod with more phosphor particles, resulting in a decrease in the output luminous flux. Meanwhile, the luminous fluxes of the yellow cylindrical rod with the surrounding transparent layer were higher than those without the transparent layer. The surrounding transparent layer redirects the blue light exiting the central cylindrical rod because of the TIR to the region away from the LD and then increases the possibility of the blue light absorption by yellow phosphor and the output power of the cylindrical rod. Furthermore, the CCTs of the cylindrical rod containing yellow phosphor with or without the surrounding transparent layer decrease with the increasing phosphor concentration. The increase in the blue laser light absorption and yellow emission from the yellow cylindrical rod was responsible for the decrease in the CCT with increasing phosphor concentration. However, the trend of the decrease in CCT with phosphor concentration is different from the decrease in yellow emissions, as illustrated in Figure 4a,b. The yellow emissions of the cylindrical rod containing yellow phosphor with or without the surrounding transparent layer initially increased with the phosphor concentration and then decreased. The high phosphor scattering prevents both the blue and yellow light from escaping the yellow cylindrical rod with more phosphor particles, resulting in a decrease in the blue and yellow emissions when phosphor concentration is high. This, in turn, leads to a decreasing CCT of the cylindrical rod containing yellow phosphor with or without the surrounding transparent layer with increasing phosphor concentration. The chromaticity coordinates of the cylindrical rod containing yellow phosphor with or without the surrounding transparent layer are displayed in Figure 4c. The CCT decreased from 11,590 to 4276 K for the

yellow cylindrical rod without the surrounding transparent layer and from 7902 to 4292 K for the yellow cylindrical rod with the surrounding transparent layer.

Table 1. Optical characteristics of the cylindrical rod containing yellow phosphor with or without surrounding transparent layer for laser-driven white lighting.

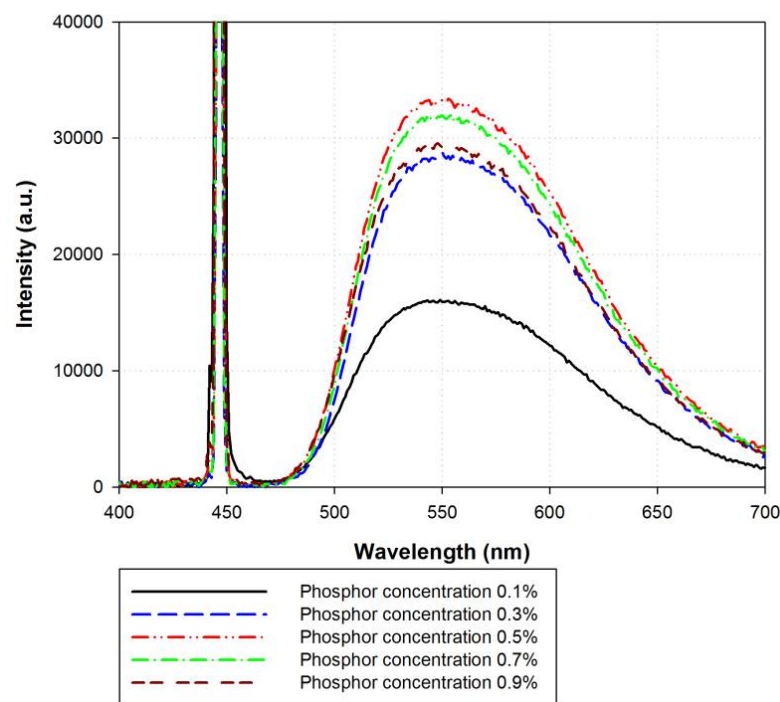
Cylindrical Rod Containing Yellow Phosphor	Phosphor Concentration (%)	CIE Coordinates (x, y)	CCT (K)	Luminous Flux (lm)
Without surrounding transparent layer	0.1	(0.2831, 0.2613)	11,590	29.9
	0.3	(0.3603, 0.4117)	4719	39.9
	0.5	(0.3761, 0.4405)	4444	42.1
	0.7	(0.3817, 0.4503)	4360	41.9
	0.9	(0.3872, 0.4574)	4276	40.7
With surrounding transparent layer	0.1	(0.3019, 0.2996)	7902	30.6
	0.3	(0.3502, 0.3922)	4946	41.4
	0.5	(0.3677, 0.4244)	4578	43.3
	0.7	(0.3782, 0.4426)	4405	42.3
	0.9	(0.3856, 0.4532)	4292	41.5

Table 2 summarizes the optical characteristics of the cylindrical rod containing both the yellow and red phosphors with or without the surrounding transparent layer and the surrounding red phosphor layer around the central yellow cylindrical rod with different Y:R ratios. At a yellow phosphor concentration of 0.5%, the CCTs of all the structures containing both yellow and red phosphors were lower than those of the cylindrical rod containing only yellow phosphor. The enhancement in the red emission of the cylindrical rod structure containing red phosphor resulted in white light emission with a low CCT. With the increasing Y:R ratios for the cylindrical rod structure, the CCT increases in the cylindrical rod containing both yellow and red phosphors with or without the surrounding transparent layer. The increase in the Y:R ratios indicates an increase in yellow phosphor weight with a corresponding decrease in red phosphor. Thus, the red emission from the red phosphor is low when the Y:R ratio is high. Furthermore, the CCT of the cylindrical rod containing both yellow and red phosphors with a high Y:R ratio was high. Moreover, the quantum yield of the red phosphor was lower than that of the yellow phosphor. In addition, the cylindrical rod containing less red phosphor (or high Y:R ratio) can cause high yellow emission with corresponding high-output power, as illustrated in Figure 5a,b. Thus, the luminous flux increases with the increasing Y:R ratio for the cylindrical rod containing both yellow and red phosphors. However, the luminous fluxes of the yellow cylindrical rod with the surrounding transparent layer were higher than those of the rod without the transparent layer. The surrounding transparent layer redirects the blue light escaping the central cylindrical rod because of the TIR to the region away from the LD and then increases the possibility of blue light absorption by the yellow and red phosphors and the output power of the cylindrical rod. Compared with the cylindrical rod containing both yellow and red phosphors with or without a transparent layer, the red phosphor layer surrounding the central yellow cylindrical rod yielded high luminous flux at different Y:R ratios. With the decrease in reabsorption in the two phosphor systems, the surrounding red phosphor layer around the central yellow cylindrical rod yielded a high luminous flux. However, most of the light emitted by the blue LD hit the yellow phosphor particles in the central yellow cylindrical rod; only part of the blue light emitting from the LD or scattered by the yellow phosphor particles hit the red phosphor particles in the surrounding red phosphor layer. The low divergence angle of the blue LD causes the low possibility of the blue light hitting the red phosphor particles in the surrounding red phosphor layer. Thus, the red emission observed in the surrounding red phosphor layer was negligible around the central yellow cylindrical rod, as illustrated in Figure 5c. Figure 5d illustrates the low variations in chromaticity coordinates and CCT of the surrounding red phosphor layer around the central yellow cylindrical rod with different Y:R ratios. The chromaticity

coordinates of the cylindrical rod containing both yellow and red phosphors with or without the surrounding transparent layer changed from natural white to warm white, which were in close proximity to the Planckian locus, as displayed in Figure 5d. The CCT increased from 2263 to 4089 K for the cylindrical rod containing both yellow and red phosphors without the surrounding transparent layer and from 2493 to 4524 K for the phosphors with the surrounding transparent layer.

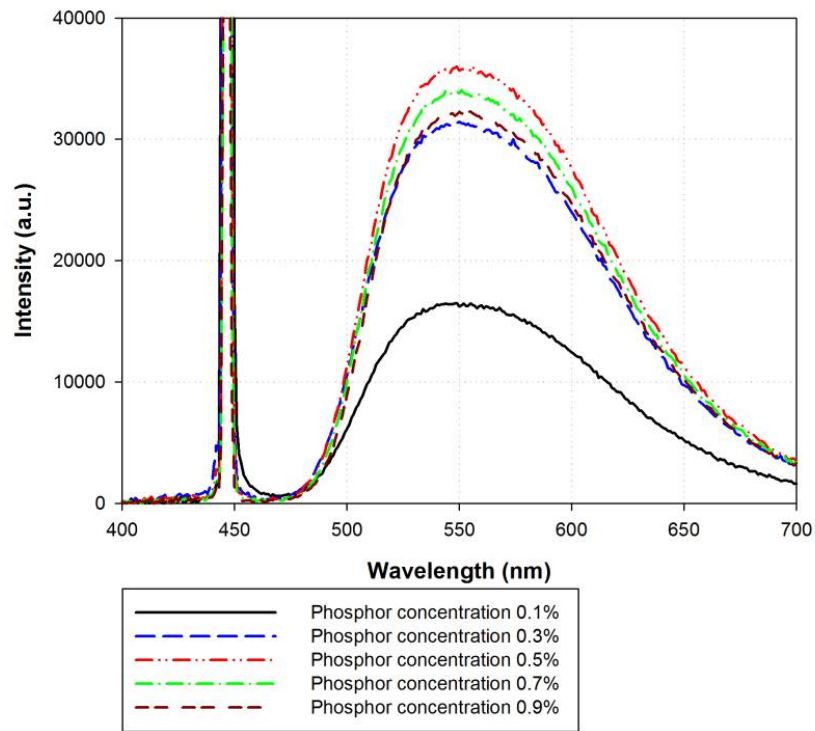
Table 2. Optical characteristics of the cylindrical rod containing both yellow and red phosphors with or without surrounding transparent layer, and the surrounding red phosphor layer around the central yellow cylindrical rod for laser-driven white lighting.

Cylindrical Rod Containing Mixed Yellow and Red Phosphors	Y:R Ratio	CIE Coordinates (x, y)	CCT (K)	Luminous Flux (lm)
Without surrounding transparent layer	3:1	(0.4591, 0.3762)	2263	29.3
	6:1	(0.4248, 0.3957)	3196	35.6
	9:1	(0.4027, 0.4022)	3695	38.0
	12:1	(0.4101, 0.3996)	3863	39.5
	15:1	(0.3946, 0.4017)	4089	41.2
With surrounding transparent layer	3:1	(0.4431, 0.3665)	2493	30.2
	6:1	(0.4103, 0.3805)	3264	36.7
	9:1	(0.3951, 0.3888)	3852	39.7
	12:1	(0.3859, 0.3902)	4096	41.1
	15:1	(0.3877, 0.3914)	4524	42.0
Surrounding red phosphor layer around central yellow cylindrical rod	3:1	(0.3915, 0.3981)	3867	37.5
	6:1	(0.3825, 0.407)	4133	40.1
	9:1	(0.3781, 0.4125)	4267	40.6
	12:1	(0.3762, 0.4142)	4321	41.4
	15:1	(0.3741, 0.4151)	4376	42.1

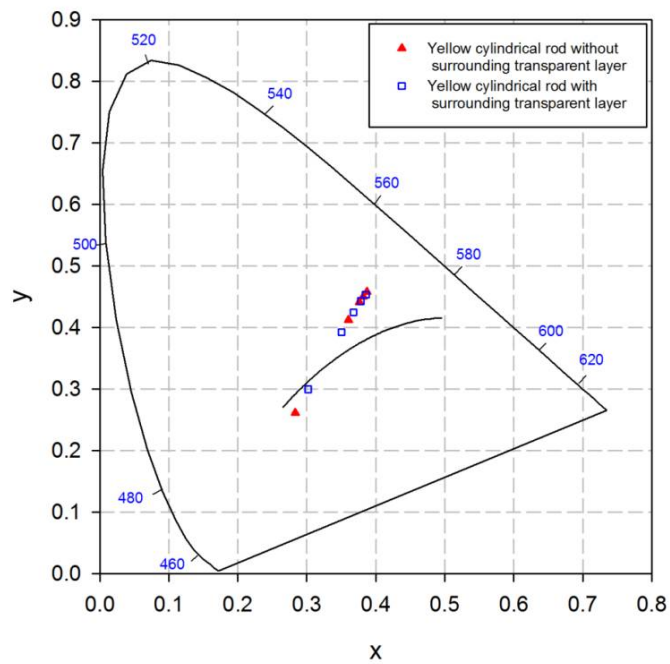


(a)

Figure 4. Cont.

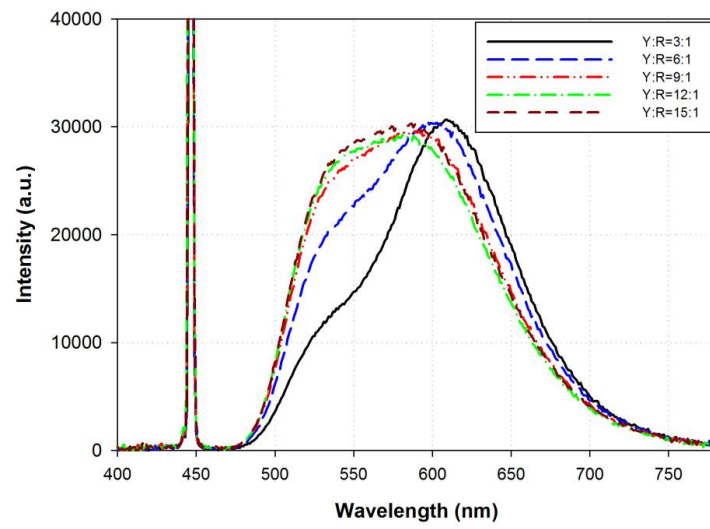


(b)

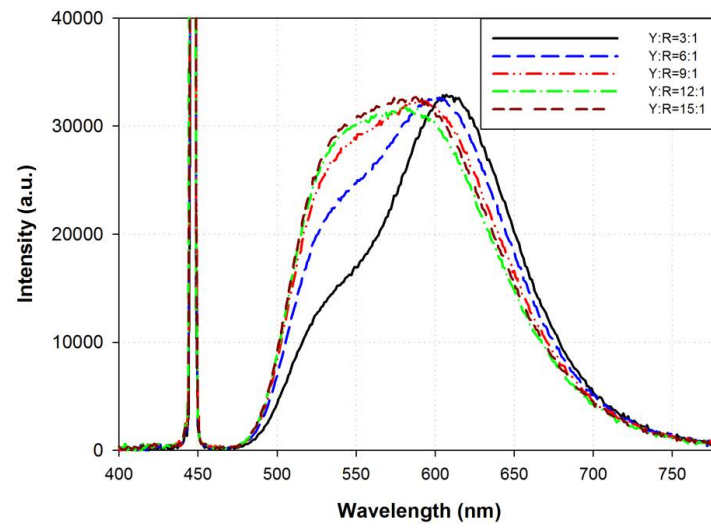


(c)

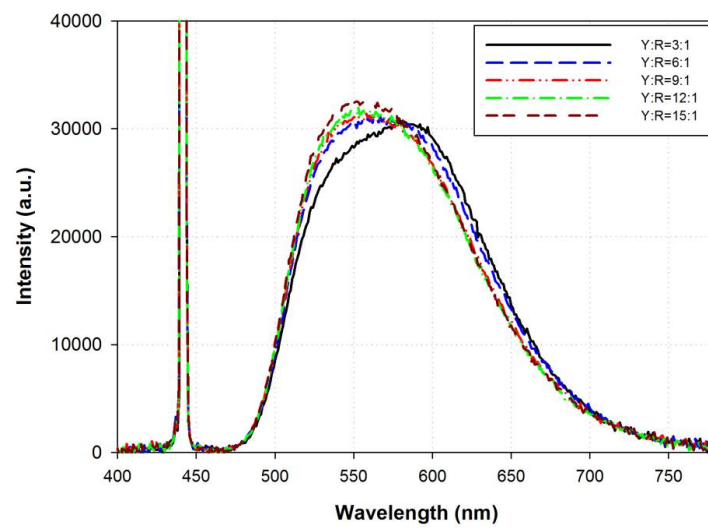
Figure 4. Emission spectra of cylindrical rod containing yellow phosphor (a) without and (b) with surrounding transparent layer for laser-driven white lighting. (c) CIE chromaticity coordinates of cylindrical rod containing yellow phosphor with or without surrounding transparent layer for laser-driven white lighting.



(a)



(b)



(c)

Figure 5. Cont.

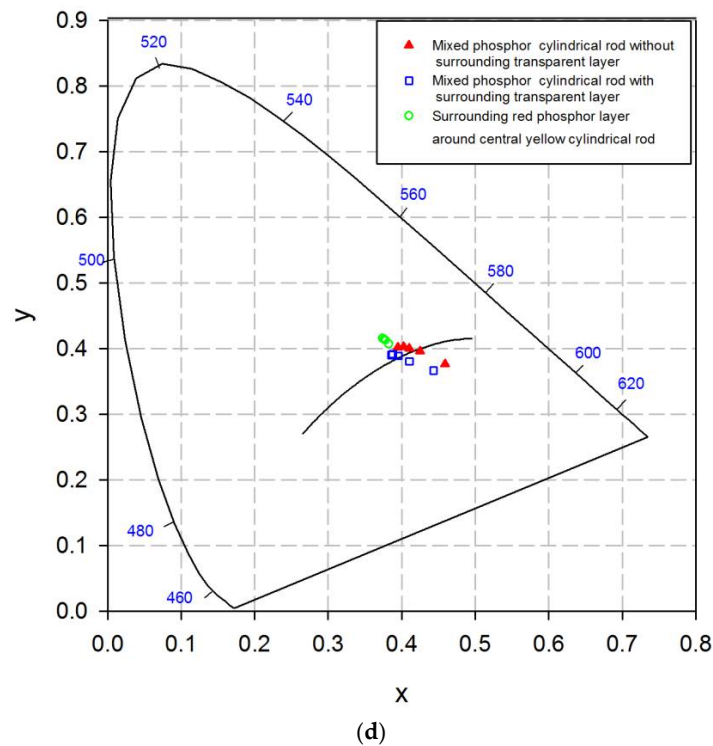


Figure 5. Emission spectra of (a) cylindrical rod containing both yellow and red phosphors without surrounding transparent layer, (b) cylindrical rod containing both yellow and red phosphors with surrounding transparent layer, and (c) surrounding red phosphor layer around central yellow cylindrical rod for laser-driven white lighting. (d) CIE chromaticity coordinates of all the samples containing both yellow and red phosphors in this study.

4. Conclusions

We demonstrated a cylindrical rod phosphor structure for laser-driven white lighting. Without the use of a focal lens, the blue light emitting from the LD with limited divergence enters the cylindrical rod containing phosphor and excites the yellow phosphor particles in the cylindrical rod to generate white light. For the cylindrical rod phosphor structure, the specific dimensions of the cylindrical rod should be determined. In this study, the FWHM values along the perpendicular and parallel transverse directions were assumed to be 23° and 6° . To enhance the usage rate of the emitting light from the LD into the cylindrical rod, the diameter of the cylindrical rod was set to 14 mm. The length of the cylindrical rod should also be specified. The scattering of the yellow phosphor in the cylindrical rod results in the scattering of the blue and yellow light propagating in the rod, thereby resulting in uniform illumination. However, the scattering of the yellow phosphor in the cylindrical rod may also prevent the blue light from the LD from exciting the phosphor particles away from the LD when the phosphor concentration is high. Thus, the specific length of the cylindrical rod was set to 50 mm. An advanced structure with a surrounding transparent layer around the central cylindrical rod containing phosphor was also investigated to enhance the possibility of the blue light absorption by yellow phosphor in the cylindrical rod region away from the LD. Furthermore, multiple phosphor blends with yellow and red phosphors were applied to the cylindrical rod phosphor structure for laser-driven, phosphor-converted white light to enhance the red luminescence of white light with a low CCT. Finally, a cylindrical rod phosphor structure with a red phosphor layer surrounding the central yellow cylindrical rod was observed. The samples with the cylindrical rod phosphor structures with or without the surrounding transparent layer were fabricated for laser-driven white lighting. For the cylindrical rod containing only yellow phosphor, the luminous fluxes of the cylindrical rod with or without the surrounding

transparent layer initially increased with the phosphor concentration and then decreased. The human eye's response to light results in an increase in luminous flux with increases at the yellow phosphor concentrations less than the threshold concentration. When the phosphor concentration is high, the high scattering of phosphor prevents the yellow light emitted by the phosphor particles from escaping the yellow cylindrical rod with more phosphor particles, thereby resulting in a decrease in the output luminous flux. Moreover, the luminous fluxes of the yellow cylindrical rod with the surrounding transparent layer were higher than those of the rods without the transparent layer. The use of the surrounding transparent layer redirects the blue light leaving the central cylindrical rod because of the TIR to the region away from the LD and then increases the possibility of the blue light absorption by yellow phosphor and the output power of the cylindrical rod. Although the maximum luminous efficiency is lower than those of other laser-driven white light structures, our structure is simpler and more compact [12,13]. We also investigated the cylindrical rod containing yellow and red phosphors with or without the surrounding transparent layer and the surrounding red phosphor layer around the central yellow cylindrical rod with different Y:R ratios. At a yellow phosphor concentration of 0.5%, the CCTs of all the structures containing both yellow and red phosphors were lower than the CCTs of the cylindrical rod containing only yellow phosphor. The luminous flux of the cylindrical rod containing both yellow and red phosphors increased with the increasing Y:R ratio. Additionally, the luminous fluxes of the yellow cylindrical rod with the surrounding transparent layer were higher than those of the rods without the transparent layer. Compared with the cylindrical rod containing both yellow and red phosphors with or without the transparent layer, the surrounding red phosphor layer around the central yellow cylindrical rod exhibited higher luminous fluxes at different Y:R ratios. However, the chromaticity coordinates and CCT variations of the surrounding red phosphor layer around the central yellow cylindrical rod with different Y:R ratios were low.

Author Contributions: Conceptualization, B.-M.C. and Y.-C.C.; methodology, S.-P.Y. and H.-L.H.; validation, B.-M.C.; formal analysis, S.-P.Y.; investigation, Y.-C.C.; data curation, H.-L.H.; writing—original draft preparation, S.-P.Y. All authors have read and agreed to the published version of the manuscript.

Funding: This research received no external funding.

Institutional Review Board Statement: Informed consent was obtained from all subjects involved in the study.

Informed Consent Statement: Not applicable.

Data Availability Statement: Not applicable.

Conflicts of Interest: The authors declare no conflict of interest.

References

1. Kim, M.-H.; Schubert, M.F.; Dai, Q.; Kim, J.K.; Schubert, E.F.; Piprek, J.; Park, Y. Origin of efficiency droop in GaN-based light-emitting diodes. *Appl. Phys. Lett.* **2007**, *91*, 183507. [[CrossRef](#)]
2. Piprek, J. Efficiency droop in nitride-based light-emitting diodes. *Phys. Status Solidi A* **2010**, *207*, 2217–2225. [[CrossRef](#)]
3. Iveland, J.; Martinelli, L.; Peretti, J.; Speck, J.S.; Weisbuch, C. Direct measurement of auger electrons emitted from a semiconductor light-emitting diode under electrical injection: Identification of the dominant mechanism for efficiency droop. *Phys. Rev. Lett.* **2013**, *110*, 177406. [[CrossRef](#)] [[PubMed](#)]
4. Wierer, J.J.; Tsao, J.Y.; Sizov, D.S. Comparison between blue lasers and light-emitting diodes for future solid-state lighting. *Laser Photon. Rev.* **2013**, *7*, 963–993. [[CrossRef](#)]
5. Liu, J.; Tam, W.S.; Wong, H.; Filip, V. Temperature-dependent light-emitting characteristics of InGaN/GaN diodes. *Microelectron. Reliab.* **2009**, *49*, 38–41. [[CrossRef](#)]
6. Neumann, A.; Wierer, J.J.; Davis, W.; Ohno, Y.; Brueck, S.R.J.; Tsao, J.Y. Four-color laser white illuminant demonstrating high color-rendering quality. *Opt. Express* **2011**, *19*, A982–A990. [[CrossRef](#)]
7. Fan, F.; Turkdogan, S.; Liu, Z.C.; Shelhammer, D.; Ning, C.Z. A Monolithic White Laser. *Nat. Nanotechnol.* **2015**, *10*, 796–803. [[CrossRef](#)]

8. Luo, X.; Fu, X.; Chen, F.; Zheng, H. Phosphor self-heating in phosphor converted light emitting diode packaging. *Int. J. Heat Mass Transf.* **2013**, *58*, 276–281. [[CrossRef](#)]
9. Yeh, C.-T.; Chou, Y.-I.; Yang, K.-S.; Wu, S.-K.; Wang, C.-C. Luminescence material characterizations on laser-phosphor lighting techniques. *Opt. Express* **2019**, *27*, 7226–7236. [[CrossRef](#)]
10. Ma, Y.; Lan, W.; Xie, B.; Hu, R.; Luo, X. An optical-thermal model for laser-excited remote phosphor with thermal quenching. *Int. J. Heat Mass Transf.* **2018**, *116*, 694–702. [[CrossRef](#)]
11. Lafont, U.; van Zeijl, H.; van der Zwaag, S. Increasing the Reliability of Solid State Lighting Systems via Self-Healing Approach: A Review. *Microelectron. Reliab.* **2012**, *52*, 71–89. [[CrossRef](#)]
12. Lee, T.-X.; Chou, C.-C.; Chang, S.C. Novel remote phosphor design for laser-based white lighting application. *SPIE Conf. Proc.* **2016**, *9954*, 96–104.
13. Chang, J.-K.; Cheng, W.-C.; Chang, Y.-P.; Kuo, Y.-Y.; Tsai, C.-C.; Huang, Y.-C.; Chen, L.-Y.; Cheng, W.-H. Next-generation glass-base phosphor-converted laser light engine. *SPIE Conf. Proc.* **2015**, *9571*, 957103.
14. Daniels, M.; Mehl, O.; Hartwig, U. Laser-activated remote phosphor light engine for projection applications. *SPIE Conf. Proc.* **2015**, *9578*, 149–155.
15. Chang, Y.-P.; Chang, J.-K.; Cheng, W.-C.; Kuo, Y.-Y.; Liu, C.-N.; Chen, L.-Y.; Cheng, W.-H. New scheme of a highly-reliable glass-based color wheel for next-generation laser light engine. *Opt. Mater. Express* **2017**, *7*, 1029–1034. [[CrossRef](#)]
16. Chen, B.-M.; Ying, S.-P.; Tsai, H.-H. Remote Phosphor Structure for Laser-Driven White Lighting. *IEEE Trans Electron Devices* **2020**, *67*, 2400–2405. [[CrossRef](#)]
17. Dubey, A.K.; Gupta, M.; Kumar, V.; Singh, V.; Mehta, D.S. Blue laser diode-pumped Ce YAG phosphor-coated cylindrical rod based extended white light source with uniform illumination. *Laser Phys.* **2019**, *29*, 056203. [[CrossRef](#)]
18. Ikeda, Y.; Takeda, Y.; Ueno, M.; Matsuba, Y.; Heike, A.; Kawasaki, Y.; Kinoshita, J. Incoherentized highbrightness white light generated using blue laser diodes and phosphors effect of multiple scattering. *J. Light Vis. Environ.* **2013**, *37*, 95–100. [[CrossRef](#)]
19. Kinoshita, J.; Ikeda, Y.; Takada, Y. Speckle-free phosphor-scattered blue light emitted out of InGaN/GaN laser diode with broadened spectral behavior for high luminance white lamp applications. *IEICE Trans. Electron.* **2013**, *96*, 1391–1398. [[CrossRef](#)]
20. Ying, S.-P.; Chien, H.-H. Effect of Reassembled Remote Phosphor Geometry on the Luminous Efficiency and Spectra of White Light-Emitting Diodes with Excellent Color Rendering Property. *IEEE Trans. Electron. Devices* **2016**, *63*, 1117–1121. [[CrossRef](#)]
21. Ying, S.-P.; Shen, J.-Y. Concentric ring phosphor geometry on the luminous efficiency of white-light-emitting diodes with excellent color rendering property. *Opt. Lett.* **2016**, *41*, 1989–1992. [[CrossRef](#)] [[PubMed](#)]
22. Lee, D.H.; Joo, J.Y.; Lee, S.K. Modeling of reflection-type laser-driven white lighting considering phosphor particles and surface topography. *Opt. Express* **2015**, *23*, 18872–18887. [[CrossRef](#)] [[PubMed](#)]